Bioresource Technology 273 (2019) 40–48

Contents lists available at ScienceDirect

Bioresource Technology

journal homepage: www.elsevier.com/locate/biortech

Performance and microbial protein expression during anaerobic treatment of alkali-decrement wastewater using a strengthened circulation anaerobic reactor

Bo Yang[a,c], Qing Wang[a], Jinshao Ye[b], Hui Xu[a], Yanbiao Liu[a,c,*], Fang Li[a,c], Xinshan Song[a,c], Jianshe Liu[a,c], Zhiwei Wang[c,d], Wolfgang Sand[a,e]

[a] Textile Pollution Controlling Engineering Center of Ministry of Environmental Protection, College of Environmental Science and Engineering, Donghua University, Shanghai 201620, China
[b] School of Environment, Jinan University, Guangzhou 510632, China
[c] Shanghai Institute of Pollution Control and Ecological Security, Shanghai 200092, China
[d] State Key Laboratory of Pollution Control and Resource Reuse, School of Environmental Science and Engineering, Tongji University, Shanghai 200092, China
[e] Institute of Biosciences, Freiberg University of Mining and Technology, Freiberg 09599, Germany

GRAPHICAL ABSTRACT

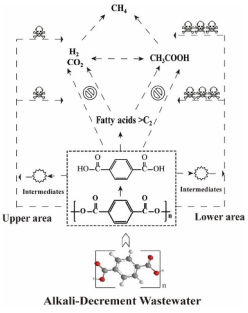

ARTICLE INFO

Keywords:
Anaerobic reactor
Alkali-decrement wastewater
Degradation mechanism
Functional metaproteome
Metabolism network

ABSTRACT

Herein, a strengthened circulation anaerobic (SCA) reactor was employed for the treatment of actual alkali-decrement wastewater. The degradation mechanism of polyester oligomers and the relationship between the treatment performance and microbial community structure were systematically investigated using various advanced techniques. Results suggest that the accumulation of volatile fatty acids has an inhibitory effect on methanogenic activity. Molecular weight distributions suggest that only incomplete degradation of oligomers was achieved, due to acetogenic inhibition in the lower part of the SCA reactor. Meta-proteomic approach analysis revealed that the methanogens containing heterodisulfide reductase were the primary species involved in methane metabolism. Based on these findings, a possible degradation mechanism for alkali-decrement wastewater in the SCA reactor is proposed. This high-performance anaerobic reactor could be further scaled-up and optimized to serve as a promising and effective unit for the treatment of other refractory industrial wastewaters.

* Corresponding author at: Textile Pollution Controlling Engineering Center of Ministry of Environmental Protection, College of Environmental Science and Engineering, Donghua University, Shanghai 201620, China.
E-mail address: yanbiaoliu@dhu.edu.cn (Y. Liu).

https://doi.org/10.1016/j.biortech.2018.10.055
Received 12 September 2018; Received in revised form 21 October 2018; Accepted 22 October 2018
Available online 29 October 2018
0960-8524/ © 2018 Elsevier Ltd. All rights reserved.

1. Introduction

Polyester is the one of the most widely used chemical fibers in the textile industry (Hasanbeigi and Price, 2015; Li et al., 2018). During typical printing and dyeing processes, alkali-decrement treatment of polyester fabric is commonly used as a pretreatment step. However, these polyester fiber surfaces can be easily hydrolyzed in sodium hydroxide solution during the treatment. This reduces the rigidity of the polyester yarn and enhances the dyeing efficiency, hygroscopicity, and permeability of the polyester fabric (Anand et al., 2014). The as-produced alkali-decrement wastewater produced is characterized by its high-concentration (> 20,000 mg/L COD), strong alkalinity (ALK), and composition of polyester hydrolysis products including sodium terephthalate, ethylene glycol, and polyester oligomers with varying degrees of polymerization (Boll et al., 2013; Manenti et al., 2015). Consequently, the characteristics of alkali-decrement wastewater are significantly different from the wastewater produced by conventional printing and dyeing (Hasanbeigi and Price, 2015).

At present, several technologies have been proposed for the treatment of alkali-decrement wastewater, including electrochemical oxidation, biological degradation, chemical precipitation, and comprehensive treatment (Jorfi et al., 2018; Zhang et al., 2018b; Zhang et al., 2017). Among them, electrochemical technologies have recently been explored for the alkali-decrement wastewater treatment. Although effective to some extent, the high operation cost, lab-scale reaction system, and potential secondary pollution have limited the wide application of such processes (Anand et al., 2014). Alternatively, the biological process has been regarded as a promising choice owing to its high efficiency and low cost (Brink et al., 2018; Cai et al., 2018; Zhao et al., 2018). For example, the alkali-decrement wastewater treatment using anaerobic baffled reactor (ABR) has been reported to show good performance (Yang et al., 2018a). The distribution of acidogenesis and methanogenesis in different ABR compartments is of importance for this system. In addition, we have recently developed a strengthened circulation anaerobic (SCA) reactor and successfully applied this to the treatment of sewage and printing and dyeing wastewater (Yang et al., 2017; Yang et al., 2018b). Results demonstrated that a two-stage reactor design facilitates a reasonable spatial distribution of acetoclastic methanogens and hydrogenotrophic methanogens along the reactor and, hence, achieves a desirable treatment performance. However, whether the SCA reactor can be successful used for the treatment of alkali-decrement wastewater is unknown. Further, most available studies on the treatment of alkali-decrement wastewater have only employed synthetic wastewater, using terephthalate acid as the main characteristic ingredient without consideration of oligomers. It is noteworthy that these oligomers are the main cause for the poor biodegradation efficacy of actual alkali-decrement wastewater (Anand et al., 2014; Wen et al., 2006).

The treatment performance of a biological system strongly depends on the activity of enzymes (Bilal et al., 2018; Chen et al., 2018). Enzymes are bioactive protein molecules that act as catalysts for certain chemical reactions in a biological system and reflect the nature of the biological process (Allen and White, 2018). The recent progress in proteomic technology provides an advanced tool to understand the complex biological process from the protein level (Schultrich et al., 2017). In an anaerobic biological treatment process, the methanogenesis as well as the metabolic processes of organic pollutants can be catalyzed by functional proteins of microbials (Ye et al., 2017; Ye et al., 2018). However, to the best of our knowledge, no reports are available on the application of a *meta*-proteomic approach into anaerobic wastewater treatment (*e.g.*, alkali-decrement wastewater). It is highly desirable to identify the functional proteins that are responsible for catalyzing the metabolism of microbials during the biological treatment process. Moreover, the essential information regarding the metabolism network regulated by enzymes is also missing.

In this study, the feasibility of an SCA reactor for the treatment of actual alkali-decrement wastewater was evaluated and the impact of several key operating parameters on the treatment performance were studied systematically. The specific objectives are to: (1) analyze the diversities and spatial distributions of the bacterial and archaeal communities within the reactor, (2) determine the functional metabolism pathways and networks related to oligomer degradation *via* an advanced *meta*-proteomic approach, and (3) propose the degradation pathways of oligomers in actual alkali-decrement wastewater. This study extends the potential applications of the SCA reactor, provides detailed information on the microbial protein expression and the metabolism of anaerobic microorganisms, and reports new insights into the treatment of actual alkali-decrement wastewater.

2. Materials and methods

2.1. Wastewater composition

The alkali-decrement wastewater was obtained as follows. A polyester fabric with a purity of 98% was subjected to a typical alkali-decrement process under high temperature (100 °C) and strong alkalinity (pH > 14). This produced a high-concentration alkali-decrement wastewater with a typical COD concentration of 60,000–70,000 mg/L mainly composed of sodium terephthalate, ethylene glycol, and polyester oligomers (Yang et al., 2018a). The wastewater was diluted further and its pH adjusted to 6.8–7.2 before use. The ALK of the water samples was adjusted using $NaHCO_3$. Trace elements and buffer were prepared according to previous reports (Dai et al., 2016; Teng et al., 2018).

2.2. Experimental set-up and sludge inoculation

A lab-scale SCA reactor with an effective capacity of 70 L was used to treat the alkali-decrement wastewater and ran for 265 days. The SCA reactor included a peristaltic pump, a primary reaction area, a secondary reaction area, and a temperature-controlled area. The schematic illustration of the SCA reactor is shown in Fig. 1 and the dimensional parameters of the SCA reactor have been detailed previously (Yang et al., 2017).

The SCA reactor was inoculated with granular sludge collected from an IC anaerobic reactor at a paper-making factory (Zhejiang Province, China). The diameter of the granular sludge ranged from 2.0 to 4.0 mm. The total inoculation volume was 28 L, which occupied 40% of the working volume of the SCA reactor. The average mixed liquor suspended solids (MLSS) level within the reactor was 19.4 g/L with a MLVSS/MLSS ratio of 0.6. The temperature was controlled at 35 ± 1 °C using an SY-2230 water bath (Crystal Technology & Industries, Inc., USA).

The whole experimental process included three periods (Periods I, II, and III). In Period I (1–60 days), certain amounts of high-concentration alkali-decrement wastewater (with a typical COD concentration of 60,000–70,000 mg/L) was added to the influent at specific times (the ratios of the alkali-decrement wastewater to the influent was 1:17 at day 1, 1:13 at day 6, 1:77 at day 16, 1:60 at day 26, 1:50 at day 36 and 1:37 at day 46). Some 200 and 100 mg/L of glucose, as co-metabolic substrate, was added to the influent at days 1 and 6 to increase the microbial activity, reduce acidification and accelerate the reactor start-up (Khan et al., 2017). The glucose was no longer added once the VFAs concentration < 300 mg/L (Huang et al., 2016). The added amounts of glucose were optimized in a previous study (Yang et al., 2018a). In Period II (61–190 days), the effects of HRT (24, 12 and 8 h) and ALK (120, 500 and 1000 mg/L) on reactor performance were systematically studied and HRT is applied to each ALK condition. In Period III (191–265 days), the impact of up-flow velocity (V_{up}, 0.1, 0.6, 0.9, 1.4 and 1.7 m/h) was further studied. The technological parameters, including HRT, runtime, COD, V_{up}, reflux ratio, ALK, and organic loading rate (OLR), are provided in Table 1.

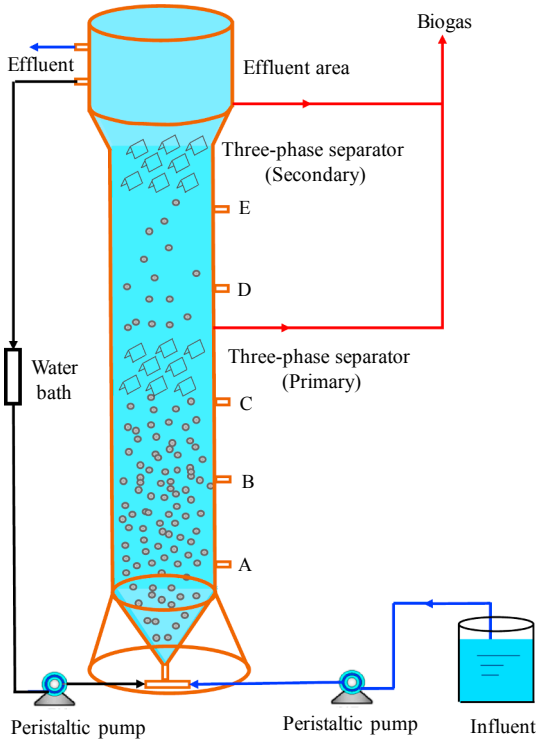

Fig. 1. Schematic representation of the strengthened circulation anaerobic (SCA) reactor.

2.3. High-throughput sequencing analysis

The seed sludge and the granular sludge were sampled from Ports A and D of the reactor for high throughput sequencing analysis in Period I and III. The DNA of the granular sludge was extracted using an OMEGA Soil DNA Kit (USA) and stored at −20 °C before use. The polymerase chain reaction (PCR) analysis was provided by Majorbio Bio-Pharm Technology Co., Ltd. (Shanghai, China). The 16S rRNA gene sequencing was conducted to identify the domain microbial populations.

2.4. Meta-proteomics analysis

A *meta*-proteomic analysis approach was developed according to a recent report (Ye et al., 2017). Briefly, proteins in seed sludge and granular sludge sampled from Ports A and D were extracted, respectively, followed by reduction with 2 μL reducing reagent in a water bath at 37 °C for 1 h. The cysteines in the proteins were blocked with 1 μL cysteine-blocking reagent for 10 min at 25 °C. After separation using a 10 kDa Amicon Ultra 0.5 mL centrifugal filter at 12,000 r/min for 20 min, the protein samples were washed with 100 μL dissolution buffer each time. The samples were then digested by 50 μL trypsin at 4% w/w 12 h at 37 °C. Subsequently, the samples were centrifuged at 12,000 r/min for 20 min and digested by 1 μg trypsin for 2 h. After centrifugation, liquid was collected in a collection tube, followed by drying in a vacuum concentrator. The samples were then resolved with a solution (consisting of 2% v/v acetonitrile and 0.1% v/v formic acid), centrifuged at 12,000 r/min for 20 min, and detected by an AB Sciex Triple-TOF 5600 mass spectrometer (AB Sciex, Framingham, MA, USA) equipped with a Nanospray III source (AB Sciex). For peptide sequence matching and protein identification, a two-step database search method was applied using a ProteinPilot™ Software 5.0 (AB SCIEX, Foster City, CA). The RAW files were first searched against the target version of a database consisting of the archaeal, bacterial and fungi proteins from UniprotKB. Accession numbers of all peptides matched in the first step were used to generate a subset FASTA database for the second step. In the second step, the RAW files were searched against a Target-Decoy version of the FASTA database. The functional metabolism pathways and network catalyzed by proteins were annotated through STRING 10.5 (http://string-db.org) and KEGG Database (http://www.kegg.jp), respectively.

2.5. Analysis methods

The COD, BOD_5, oxidation-reduction potential (ORP), pH, ALK, SS, VSS and UV_{254} were determined following standard methods (Apha, 2005). Volatile fatty acids (VFAs) were measured by titration (Wijetunga et al., 2010). At the end of each period, granular sludge samples were collected and analyzed for dehydrogenase (DHA) and coenzyme F_{420}. The analyses of DHA and coenzyme F_{420} have been described previously (Yang et al., 2018b). The molecular weight distributions of the samples were determined *via* a reported filtration assay (Su et al., 2018). Samples were collected from the influent, the effluent,

Table 1
Operational parameters for the SCA reactor during the treatment of alkali-decrement wastewater.

Period	HRT (h)	Time (d)	Influent COD (mg/L)	Influent BOD_5 (mg/L)	Influent TSS (mg/L)	V_{up} (m/h)	Reflux velocity (L/h)	Reflux ratio	Alkalinity (mg/L)	Average OLR (kg COD/m^3/d)
I	24	5	500–600	150–200	35–150	0.14	1.46	0.50	1000	0.57
		10	700–800	185–210						0.77
		10	900–1000	250–310						0.98
		10	1000–1100	255–330						1.08
		10	1300–1400	350–410						1.39
		15	1700–2000	510–620						1.91
II	24	10	1800–2500	540–750	80–180	0.5	12.78	4.38	120	2.21
		15				1.0	28.48	9.77	500	
		15				2.0	59.88	20.53	1000	
	12	15				1.0	28.48	9.77	120	
		15				2.0	59.88	20.53	500	
		15				0.5	12.78	4.38	1000	
	8	15				2.0	59.88	20.53	120	
		15				0.5	12.78	4.38	500	
		15				1.0	28.48	9.77	1000	
III	24	15	1100–2000	320–620	70–150	0.1	0.00	0.00	500	1.39
		15				0.6	15.92	5.46		
		15				0.9	25.34	8.69		
		15				1.4	40.00	13.00		
		15				1.7	50.00	19.00		

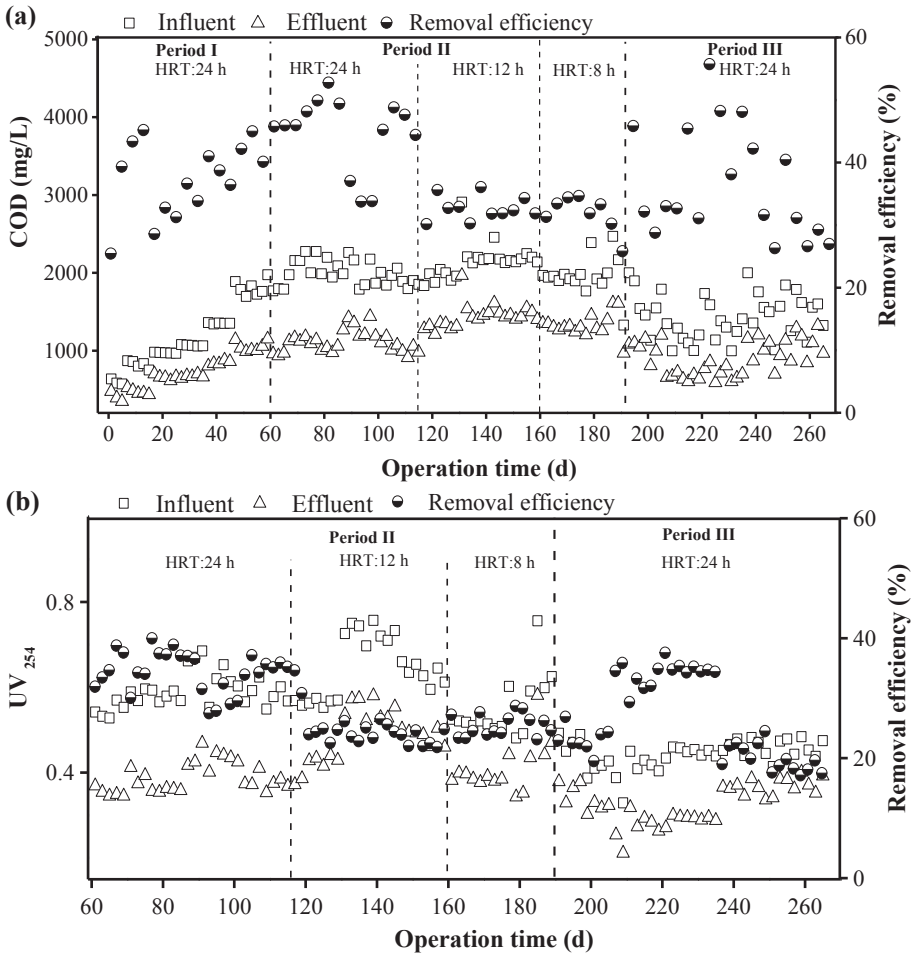

Fig. 2. Variations in (a) COD concentration and COD removal efficiency, and (b) UV_{254} and UV_{254} removal efficiency in influent and effluent samples.

and all the sampling ports during Period III. Motimo ultrafiltration membranes (Tianjin, China) with molecular weight cut-offs (MWCFs) of 300–600 Da and 150–300 Da were used to separate the organics from the liquid with a typical pressure of 0.15–0.25 MPa. After filtration, the concentration of organic compounds was characterized by COD and UV_{254} determination.

3. Results and discussion

3.1. Performance of the SCA reactor

Fig. 2a presents the COD removal performance of the SCA reactor as a function of operation time and HRT. During the start-up phase of the reactor, *i.e.*, Period I (1–60 days), a certain amount of glucose was added to the alkali-decrement wastewater to enhance the biodegradability and shorten the start-up time. The influent COD concentration was 500–800 mg/L and the COD removal efficiency increased quickly from 25.4% to 47.4% within the initial 9 days, indicating a successful start-up of the reactor. When the influent COD concentration was further raised to 1000 mg/L, glucose was no longer spiked. Consequently, the COD decreased initially to 31.4%, then gradually increased and remained stable. During Period II (61–190 days), the influent COD concentration varied from 1800 to 2500 mg/L, while the COD removal efficiency varied between 30.7% and 50.0% during the operation. Optimal performance was obtained under operational conditions of HRT = 24 h and ALK = 500 mg/L. In Period III (191–265 days), the V_{up} of 0.1, 0.6, 0.9, 1.4 and 1.7 m/h were compared, and the SCA reactor ran for 15 days at each V_{up} condition. The effluent COD removal efficiency increased from 32.2% to 48.6% with the V_{up} increasing from 0.1 to 0.9 m/h (see Fig. 2 and Table 1). However, further increasing the V_{up} to 1.4 and 1.7 m/h contributed negatively to COD removal. In addition, the effluent COD concentration collected from different sampling ports (*e.g.*, A, B and D) along the reactor height were also monitored to evaluate the SCA reactor's performance. The results suggest that the COD removal efficiency increased along the SCA reactor height, and the effluent COD concentration at Port D decreased clearly compared with the other ports.

It has been reported that co-substrates can be used as electron donors to promote the degradation of pollutants with poor biodegradability (Fortela et al., 2016; Liu et al., 2014). Indeed, the COD removal was evidently improved by adding glucose as a co-substrate in this study. The HRT is another important parameter of the anaerobic reactor system. Typically, an increased HRT guarantees stable COD removal due to an extended contact time for the biomass and the organics. Herein, a HRT of 24 h was identified as optimal. Besides, an appropriate V_{up} enhances the mass transfer within the reactor, guarantees sufficient wastewater-biomass contact within the reactor, and facilitates organic removal and sludge stabilization. This can also be reflected by the increase of coenzyme F_{420} and DHA concentrations with V_{up}. However, an excessive V_{up} decreases COD removal performance and leads to a disintegration of the granular sludge. Compared to sampling Ports A and B, Port D showed significantly better COD removal efficiency, despite the highest DHA activity at Port B. This is likely due to the presence of three-phase separators inside the SCA reactor. On the one hand, these separators can effectively avoid the intermixing of sludge from the lower and upper parts of the reactor; on the other hand, the middle three-phase separators in the two-stage reactor design are beneficial to the local mixing of liquid and solid phases within either

the lower or upper parts of the reactor.

Aromatic compounds (aromatic hydrocarbons with double bonds or carboxyl groups) have strong absorption in the UV range, while saturated low-grade fatty acids and amino acids demonstrate negligible absorption in this range (Haider et al., 2002; He et al., 2014). Thus, UV_{254} was employed to characterize the contents of the aromatic compounds in the wastewater during Periods II and III. As shown in Fig. 2b, the change in UV_{254} had a similar trend to that for COD. Specifically, the UV_{254} removal efficiency in Period II was in the range of 23.2–40.0%. The microbial metabolism requires more time to degrade these oligomers in alkali-decrement wastewater which, in turn, results in an increased HRT (*e.g.*, 24 h). During Period III, a limited UV_{254} removal rate of 22.5% was obtained at a V_{up} of 0.1 m/h. Then, UV_{254} removal gradually increased with V_{up} up to 0.9 m/h, at which point the maximum removal efficiency of 35.2% was observed. Further increasing V_{up} to 1.7 m/h resulted in a lower removal rate of 17.2%. Similarly, UV_{254} removal increased with reaction time, and the highest removal efficiency was obtained at sampling Port D, compared with Ports A and B.

3.2. Molecular weight distribution of the wastewater

The molecular weight distribution of wastewater sampled from different effluent ports was determined to further verify the degradation of alkali-decrement wastewater. The wastewater was collected from different sampling ports and separated *via* an ultrafiltration membrane with MWCFs of < 150 Da, 150–300 Da, 300–500 Da, 500–600 Da, and > 600 Da, respectively. The variation in molecular weight distributions along the SCA reactor is summarized in Fig. 3a. The COD concentration gradually decreased in the reactor. > 40% of the influent possessed a molecular weight of > 600 Da with a typical COD concentration of 739 ± 23 mg/L. The COD concentration decreased to 346 ± 16 mg/L with a COD removal efficiency of 53.2% at Port C. However, the COD concentration changed negligibly from Port C to Port E in terms of molecular weights > 600 Da. This indicates that these large compounds were degraded by hydrolysis and acidification in the lower part of the reactor. This is consistent with the change of enzyme activity discussed above. Although the molecular weight distributions changed, the total COD concentration remained almost constant at Ports C, D and E. This suggests that the degradation of aromatic compounds was insufficient in the upper part of the SCA reactor.

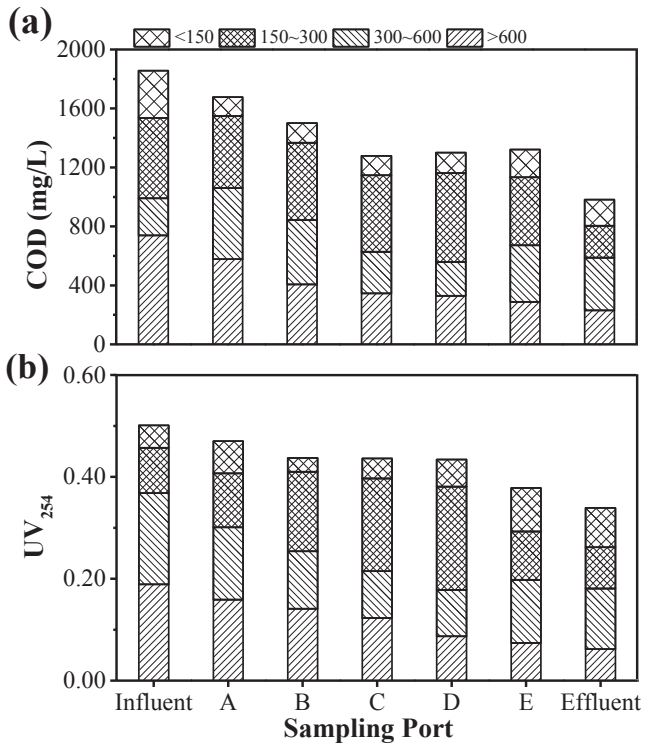

Fig. 3. Variations in the molecular weight distributions of wastewater sampled from different reactor ports, as measured by (a) COD, and (b) UV_{254}. Experimental conditions: HRT = 24 h, ALK = 500 mg/L and V_{up} = 0.9 m/h.

The molecular weight distribution of wastewater sampled from different ports in the reactor was also analyzed with UV_{254}. As shown in Fig. 3b, the UV_{254} absorption gradually decreased along the reactor height, but its decrease was less than that for COD. Besides, a continuous downward trend was observed for compounds with molecular weights > 600 Da. This suggests that the degradation rate of aromatic compounds is lower than that for non-aromatic compounds. In addition, small compounds with molecular weights of 150–300 Da can be further degraded, while larger ones are resistant to degradation. The proportion of compounds with molecular weights < 150 Da was not reduced in the reactor. This may be attributable to the existence of persistent small molecular pollutants in the wastewater. As described previously, the degradation of organic matter in the reactor requires the involvement of syntrophs and methanogens. The conversion of aromatic compounds to acetate is energetically unfavorable (*e.g.*, $terephthalate^{2+} + 8H_2O \rightarrow 3\,acetate^- + 3H^+ + 2HCO_3^- + 3H_2$, $\triangle G = +38.9$ kJ/moL) and needs to be coupled with a methanogenic reaction ($HCO_3^- + 4H_2 + H^+ \rightarrow CH_4 + 3H_2O$, $\triangle G = -135.6$ kJ/moL and/or $3acetate^- + H_2O \rightarrow CH_4 + HCO_3^-$, $\triangle G = -31.0$ kJ/moL) to proceed further (Boll et al., 2013). This may explain why the degradation of aromatic compounds remained incomplete in the SCA reactor. Because the acetogenic reaction is probably suppressed at the lower part of the reactor, the degradation of aromatic compounds is inhibited. However, such inhibition is relieved at the upper part of the reactor, so that the aromatic compounds can be degraded.

3.3. Analyses of the microbial community in granular sludge

Three microbial samples (raw sludge, sludge at Ports A and D) were collected to analyze the biodiversity of bacteria and archaea (Table 2). The richness parameter for bacteria revealed an obvious growth after inoculation. In addition, the richness of bacteria in samples at Port A was slightly lower than that at Port D. However, the richness of archaea at Port A was almost the same as that of the raw sludge. An increasing trend for this value from Port A to Port D was observed. The richness and evenness of the microbial diversity were evaluated by the Shannon and Simpson coefficients. There were no fluctuations in the Shannon and Simpson coefficients of bacteria, but decreasing trends were noted for archaea. A high concentration of influent promotes microbial growth. The toxicity of wastewater gradually decreased during its passage through the reactor due to metabolization by microorganisms. This may explain the increasing trend in the richness coefficients for archaea and bacteria from the lower to the upper parts of the reactor.

Trichococcus and *norank_c_Bacteroidetes_vadinHA17* were the dominant genera in the samples from Ports A and D, which are significantly different from that in the raw sludge bacterial community.

Table 2
Richness and evenness of bacteria and archaea in sludge samples from the SCA reactor.

Microbes	Sample	Coverage	ACE	Chao	Shannon	Simpson
Bacteria	Inoculation	0.999	254.49	257.23	3.621	0.064
	A#	0.999	348.13	355.00	3.681	0.083
	D#	0.999	361.13	365.94	3.652	0.075
Archaea	Inoculation	1.000	18.00	18.00	1.151	0.539
	A#	0.999	17.50	18.00	0.961	0.445
	D#	0.999	20.00	21.00	0.912	0.478

Methanosaeta (76.8%) and *Methanolinea* (10.7%) were found to be the dominant archaeal genera in the raw sludge sample. However, the dominant *Methanolinea* was replaced by *Methanobacterium* after inoculation of the raw sludge. The relative abundance of *Methanosaeta* increased from the lower to the upper part of the SCA reactor, whereas that for *Methanobacterium* decreased. Obviously, only a limited number of organisms can metabolize the aromatic compounds under anaerobic conditions. These microorganisms included the syntrophs (*e.g.*, *Syntrophorhabdus, Syntrophus* and *Pelotomaculum*) and methanogens (*e.g.*, *Methanosaeta, Methanosarcina, Methanolinea, Methanospirllum,* and *Methanobacterium*) (Covino et al., 2016; Gerrity et al., 2018; Kato et al., 2015). After inoculation, an evident change in the abundances of *Synergistetes*, *Thermotogae*, *Firmicutes*, and *Actinobacteria* was observed. The largest archaeal group are the *Methanosaeta*, which belong to the acetoclastic methanogens and compete with hydrogenotrophic methanogens (*e.g.*, *Methanolinea* and *Methanobacterium*) (Xu et al., 2018). However, the acetoclastic methanogens (*Methanosaeta*) were the dominant species in all cases, and the abundance of hydrogenotrophic methanogens (*Methanobacterium*) decreased during reactor passage.

3.4. Degradation mechanism for alkali-decrement wastewater

During the degradation of aromatic compounds in alkali-decrement wastewater, the production of intermediates and/or characteristic pollutants inhibits the degradation performance. This may lead to incomplete degradation of aromatic compounds in the SCA reactor. However, this inhibition may be gradually relieved during the passage through the reactor. The dynamic change in the microbial community structure was analyzed by high-throughput sequencing to explore these key microbial flora (syntrophs and methanogens) for the degradation of the aromatic compounds in the SCA reactor. The results revealed that an evident change in the abundances of *Synergistetes*, *Thermotogae*, and *Firmicutes* was observed after inoculation. Among these have been identified as significant contributors to the degradation of aromatic compounds (Li et al., 2018; Yang et al., 2018b). Further, the largest archaeal group are the acetoclastic methanogens (*Methanosaeta*) that were the dominant species in both the lower and upper parts (Lu et al., 2018). However, the abundance of hydrogenotrophic methanogens (*Methanobacterium*) decreased during reactor passage. This result is different from our previous reports (Yang et al., 2017; Yang et al., 2018b), suggesting that the acetogenic reaction, in this case, was probably restrained at the lower part of the reactor for the treatment of alkali-decrement wastewater. Such an inhibitory effect was relieved in the upper part due to the presence of sufficient VFAs for the acetogenic reaction. This explains why a significant enhancement of SMA and coenzyme F_{420} was measurable along the reactor. Thus, we postulate that the bacteria responsible for VFA degradation *via* producing acetic acid were inhibited due to the existence of toxic intermediates and/or characteristic pollutants in the lower part of the reactor. This implies that the degradation of aromatic compounds was incomplete, because the methanogenic reaction could only proceed slowly. However, these toxic intermediates and/or characteristic pollutants become gradually metabolized and/or diluted during the passage through the reactor. Consequently, the acetogenic reaction and methanogenic reaction can proceed in the upper part of the reactor. Based on this finding, we propose a possible degradation mechanism for alkali-decrement wastewater in SCA reactor (Fig. 4). The two main microbial flora types (syntrophs and methanogens) are essential for the degradation of aromatic compounds in an SCA reactor.

3.5. Analyses of the functional metaproteome and metabolism networks

With at least two peptides matched with > 95% confidence, 1011, 1270, and 1115 of proteins extracted from the seed sludge, and sludge collected at Ports A and D, respectively, were identified. Based on their molecular functions, the percentages of each *meta*-proteome dataset exhibited certain variations. Compared to the seed sludge, 274 and 176 proteins were found only expressed in samples from ports A and D. This finding confirmed the different expressions of the functional proteins and the succession of microbes during the anaerobic treatment process, which is consistent with the results of the microbial community in granular sludge. After pollutant treatment, metaproteomes in samples were differentially expressed.

3.5.1. Protein-protein interaction

To clarify the relationships between functional proteins in the anaerobic conditions, the interaction among proteins expressed in methanogens was analyzed. Among the identified proteins in the granular sludge at Port D, 381 of them were found to be expressed by methanogens through String analysis (https://string-db.org) and the results are displayed in Fig. 5. Approximately half of these multifunctional proteins were significantly enriched in 23 metabolism pathways (Table S1). Based on the protein interactions, functional proteins in the ribosome pathway were directly connected with the proteins regulating purine metabolism and oxidative phosphorylation. V-type ATP synthase subunit D (atpD), responsible for producing ATP from ADP in the presence of a proton gradient across a cellular membrane, is one of the key node proteins for their connection (Mulkidjanian et al., 2007). The precursors produced in the purine metabolism process were used to synthesize proteins regulating the biosynthesis of amino acids. Some of these amino acids were precursors for the generation of proteins catalyzed by methane and nitrogen metabolism. Oxidative phosphorylation is the key node pathway connected with regulated purine metabolism and methane metabolism.

3.5.2. Methane metabolism network

To reveal the detailed chemical reactions catalyzed by the functional enzymes and the regulated pathways related to the metabolism of syntrophs and methanogens, the metabolism network regulated by those enzymes was determined, as displayed in Fig. 6. In the pathway of methane metabolism, carbon dioxide was transformed by acetyl-CoA decarbonylase (EC:1.2.7.4, ACDS) with the production of 5,6,7,8-tetrahydromethanopterin (THMPT), which is a carrier of the C1 group in methanogenesis. THMPT further donated the C1 group to coenzyme M. As the enzyme catalyzed the final step in methane formation, coenzyme-B sulfoethylthiotransferase (EC:2.8.4.1) received the methyl group to generate methane. The enzymatic activity of coenzyme-B in sludge sampled at Ports A and D was recovered through the reversible reduction of CoM-S-S-CoB to coenzyme M and coenzyme B catalyzed by heterodisulfide reductase [EC:1.8.98.1] (Yan et al., 2018). Meanwhile, this reversible reduction in the seed sludge was catalyzed by enzymes EC:1.8.7.3, 1.8.98.1, 1.8.98.4, 1.8.98.5, and 1.8.98.6. This finding confirmed that, although there were different species of microbes in the seed sludge, only those with the high activity of EC:1.8.98.1 were enriched in the anaerobic reactor during the treatment of alkali-decrement wastewater.

Methylene tetrahydromethanopterin dehydrogenase [EC:1.5.98.1], coenzyme F_{420} hydrogenase subunit alpha [EC:1.12.98.1] and 5,10-methylenetetrahydromethanopterin reductase [EC:1.5.98.2] were involved in the transformation of coenzyme F_{420}. Consequently, reduced F_{420} concentrations were witnessed. These findings confirm that methane metabolism occurred during the degradation of the alkali-decrement wastewater.

3.5.3. Organic acid metabolism

Acetyl-CoA was another key node in the metabolism network regulated by functional proteins in the sludge samples. It connected the citrate cycle with amino acid metabolism, and generated acetate with catalysis by acetyl-CoA synthetase (EC:6.2.1.1). Acetoacetate-CoA ligase (EC:6.2.1.12) is an enzyme that was only found in the sample at port D, and it catalyzed the chemical reaction (2). Acetoacetyl-CoA could further transform to acetyl-CoA by the catalysis of enzymes (EC:

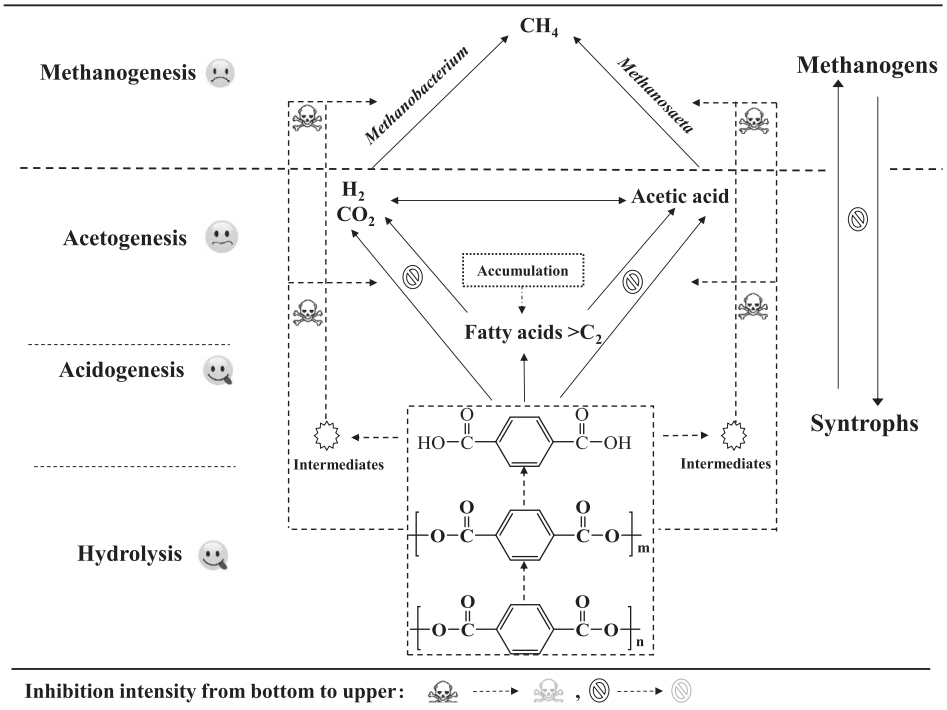

Fig. 4. Schematic illustration of the metabolic steps of alkali-decrement wastewater degradation by the SCA reactor.

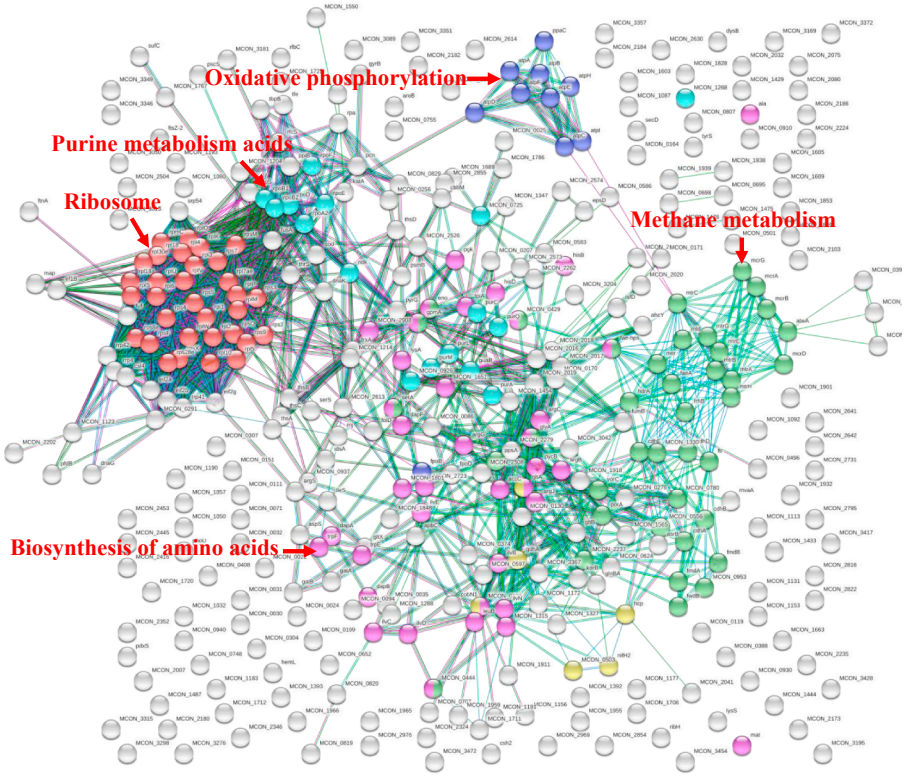

Fig. 5. Interaction among functional proteins regulating methane metabolism and other proteins in granular sludge sampled from Port D.

2.3.1.9). These results mean the low production of acetate and acetoacetate in port D, which is consistent with the inhibited generation of acetate because of the low concentration of coenzyme F_{420}.

$$\text{ATP} + \text{acetoacetate} + \text{CoA} <=> \textit{AMP} + \textit{diphosphate} + \textit{acetoacetyl} - \textit{CoA} \quad (2)$$

A series of alcohol dehydrogenases (EC:1.1.1.1) were expressed in the sludge samples. They were transformed from 3-chloroallyl alcohol to 3-chloroallyl aldehyde, facilitating the interconversion between 2-naphthalenemethanol and 2-naphthaldehyde, and catalyzing ethyne to ethylene in the chloroalkane and chloroalkene degradation pathway (Zhang et al., 2018a). Transformation of 1-hydroxymethylnaphthalene

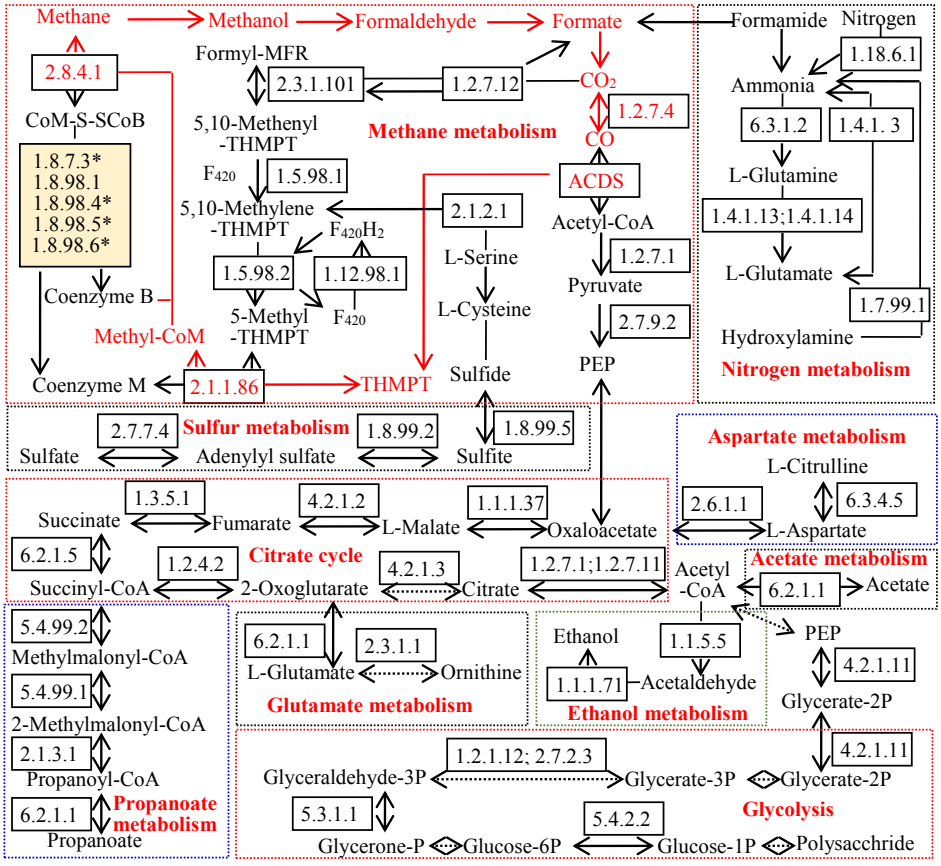

Fig. 6. Methane, nitrogen and organic acid metabolism regulated by the functional proteins in the seed sludge and granular sludge (* denotes unique enzymes only found in the seed sludge).

to 1-naphthaldehyde via the aromatic compound degradation pathway was observed in the sludge samples. Moreover, the degradation of benzoate catalyzed by acylphosphatase (EC 3.6.1.7) was also determined. These findings are direct evidence of how the alkali-decrement wastewater was degraded within the reactor. The transformation of 1-alcohol to aldehyde catalyzed by alcohol dehydrogenase, and the chemical reaction of glutaryl-CoA to glutaconyl-CoA regulated by glutaryl-CoA dehydrogenase (EC:1.3.99.32) in the fatty acid degradation pathway, clarify why VFAs were generated.

3.5.4. Chemotaxis and substrate transport

Chemotaxis is the movement of motile bacteria based on chemical gradients sensing through methyl-accepting chemotaxis proteins (Hida et al., 2015). During the chemotaxis process, protein CheB removed methyl groups from glutamate residues on the cytosolic side of the receptor. CheB works antagonistically with a methyltransferase, which adds methyl residues to the same glutamate residues, resulting in the methylation of the methyl-accepting chemotaxis proteins. No chemotaxis protein was found in the seed sludge, whereas, methyl-accepting chemotaxis sensory transducer and chemotaxis proteins were detected in the sludge of port D. These results mean that during the process of alkali-decrement wastewater treatment, some functional proteins involved in chemical gradients sensing were synthesized by microbes for the binding and transport of the target substrates.

The expression of ferric uptake regulation protein Fur, nitrite transporter NirC, high-affinity carbon uptake protein Hat, oligopeptide/dipeptide ABC transporter, peptide ABC transporter substrate-binding protein, multidrug ABC transporter ATP-binding protein, amino acid ABC transporter permease, cobalamin biosynthesis protein CobN and MFS transporter clarifies that the binding and transport of metal ion, peptide, xenobiotics, amino acids and small solutes by functional proteins expressed in bacteria in port D were upregulated compared to the seed sludge.

Among these functional proteins, Fur is responsible for regulating metal ion uptake and for metal homeostasis. Peptide transporters are primarily involved in the transport of small peptides with the concomitant intake of protons. CobN is a subunit of cobalt chelatase for cobalamin biosynthesis and the transport of cobalt and magnesium. MFS transporter facilitated the movement of small solutes across cell membranes in response to chemiosmotic gradients. Based on the sequencing analysis, multidrug ABC transporter ATP-binding protein has some motifs related to the transport of heavy metals and toxins. Another two functional proteins, TetR family transcriptional regulator and membrane protein, involved in aromatic hydrocarbon degradation were also related to pollutant transport. TetR plays an important role in conferring xenobiotics resistance to many bacterial species (Arzamasov et al., 2018). It represses the synthesis of TetA, a protein that pumps out toxic substances, by binding the TetA operator. Their expression means that the transport of pollutants by microbes in port D was activated compared to the seed sludge.

In the sludge of Port A, methyl-accepting chemotaxis PctC and methyltransferase were found. The synthesis of sugar ABC transporter ATP-binding protein, amino acid ABC transporter substrate-binding protein, ferric enterobactin receptor, peptide/nickel transport system substrate-binding protein, multiple sugar transport system ATP-binding protein, iron-regulated ABC transporter permease protein SufD, oligopeptide transport system permease protein OppB, multidrug ABC transporter substrate-binding protein, biopolymer transport protein ExbB, calcium-transporting ATPase, cation transporter, urea transport system ATP-binding protein and peptide ABC transporter ATP-binding protein in bacteria in port A revealed that the transport of sugar, amino acids, peptide, urea, xenobiotics and metal ions was activated.

4. Conclusions

In this study, an SCA reactor was employed to treat alkali-decrement wastewater over 265 days. Analyses of the molecular weight distributions and of enzyme activities demonstrated that the inhibition of acetogenic reactions was the main reason for the incomplete degradation of aromatic compounds. High-throughput sequencing analysis indicated that the two main players in the microbial flora (syntrophs and methanogens) were essential for the degradation of the aromatic compounds. Methanogens with heterodisulfide reductase for the reduction of coenzyme B were the primary species for methane metabolism, which is related to nitrogen metabolism, sulfur metabolism and energy metabolism.

Acknowledgements

This work was supported by the National Key Research and Development Program of China (No. 2018YFF0215703 and No. 2016YFC0400501), the National Science Foundation of China (21876064), the Shanghai Science and Technology Committee (No. 17DZ1202204), the Shanghai Pujiang Program (No. 18PJ1400400), and the Natural Science Foundation of Shanghai, China (No. 18ZR1401000). Y.L. thanks Donghua University for the start-up grant (No. 113-07-005710).

Appendix A. Supplementary data

Supplementary data to this article can be found online at https://doi.org/10.1016/j.biortech.2018.10.055.

References

Allen, K.D., White, R.H., 2018. Identification of the Radical SAM Enzymes Involved in the Biosynthesis of Methanopterin and Coenzyme F420 in Methanogens. In: Methods in Enzymology. Academic Press, pp. 461–483.
Anand, M.V., Srivastava, V.C., Singh, S., Bhatnagar, R., Mall, I.D., 2014. Electrochemical treatment of alkali decrement wastewater containing terephthalic acid using iron electrodes. J. Taiwan Inst. Chem. Eng. 45 (3), 908–913.
Apha, A. 2005. WEF, Standard methods for the examination of water and wastewater. 21, 258-259.
Arzamasov, A.A., van Sinderen, D., Rodionov, D.A., 2018. Comparative genomics reveals the regulatory complexity of bifidobacterial arabinose and arabino-oligosaccharide utilization. Front. Microbiol. 9 (776).
Bilal, M., Iqbal, H.M.N., Hu, H., Wang, W., Zhang, X., 2018. Metabolic engineering and enzyme-mediated processing: a biotechnological venture towards biofuel production–a review. Renew. Sustain. Energy Rev. 82, 436–447.
Boll, M., Loffler, C., Morris Brandon, E.L., Kung Johannes, W., 2013. Anaerobic degradation of homocyclic aromatic compounds via arylcarboxyl-coenzyme A esters: organisms, strategies and key enzymes. Environ. Microbiol. 16 (3), 612–627.
Brink, A., Sheridan, C., Harding, K., 2018. Combined biological and advance oxidation processes for paper and pulp effluent treatment. S. Afr. J. Chem. Eng. 25, 116–122.
Cai, W., Jin, M., Zhao, Z., Lei, Z., Zhang, Z., Adachi, Y., Lee, D.-J., 2018. Influence of ferrous iron dosing strategy on aerobic granulation of activated sludge and bioavailability of phosphorus accumulated in granules. Bioresour. Technol. Rep. 2, 7–14.
Chen, K., Zhao, Z., Yang, X., Lei, Z., Zhang, Z., Zhang, S., 2018. Desorption trials and granular stability of chromium loaded aerobic granular sludge from synthetic domestic wastewater treatment. Bioresour. Technol. Rep. 1, 9–15.
Covino, S., Fabianova, T., Kresinova, Z., Cvancarova, M., Burianova, E., Filipova, A., Voriskova, J., Baldrian, P., Cajthaml, T., 2016. Polycyclic aromatic hydrocarbons degradation and microbial community shifts during co-composting of creosote-treated wood. J. Hazard. Mater. 301, 17–26.
Dai, R., Chen, X., Luo, Y., Ma, P., Ni, S., Xiang, X., Li, G., 2016. Inhibitory effect and mechanism of azo dyes on anaerobic methanogenic wastewater treatment: can redox mediator remediate the inhibition? Water Res. 104, 408–417.
Su, Z., Luo, J., Pinelo, M., Wan, Y., 2018. Directing filtration to narrow molecular weight distribution of oligodextran in an enzymatic membrane reactor. J. Membr. Sci. 555, 268–279.
Fortela, D.L., Hernandez, R., Chistoserdov, A., Zappi, M., Bajpai, R., Gang, D., Revellame, E., Holmes, W., 2016. Biodiesel profile stabilization and microbial community selection of activated sludge feeding on acetic acid as a carbon source. ACS Sustainable Chem. Eng. 4 (12), 6427–6434.
Gerrity, D., Arnold, M., Dickenson, E., Moser, D., Sackett, J.D., Wert, E.C., 2018. Microbial community characterization of ozone-biofiltration systems in drinking water and potable reuse applications. Water Res. 135, 207–219.
Haider, T., Sommer, R., Knasmuller, S., Eckl, P., Pribil, W., Cabaj, A., Kundi, M., 2002. Genotoxic response of Austrian groundwater samples treated under standardized UV (254nm)—disinfection conditions in a combination of three different bioassays. Water Res. 36 (1), 25–32.
Hasanbeigi, A., Price, L., 2015. A technical review of emerging technologies for energy and water efficiency and pollution reduction in the textile industry. J. Cleaner Prod. 95, 30–44.
He, X., Mezyk, S.P., Michael, I., Fatta-Kassinos, D., Dionysiou, D.D., 2014. Degradation kinetics and mechanism of β-lactam antibiotics by the activation of H_2O_2 and $Na_2S_2O_8$ under UV-254nm irradiation. J. Hazard. Mater. 279, 375–383.
Hida, A., Oku, S., Kawasaki, T., Nakashimada, Y., Tajima, T., Kato, J., 2015. Identification of the mcpA and mcpM Genes Encoding Methyl-Accepting Chemotaxis Proteins (MCPs) for Amino Acids and L-Malate and Involvement of McpM-mediated Chemotaxis in Plant Infection by Ralstonia pseudosolanacearum (Ralstonia solanacearum). Appl. Environ. Microbiol. 81 (21), 7420–7430.
Huang, W., Huang, W., Yuan, T., Zhao, Z., Cai, W., Zhang, Z., Lei, Z., Feng, C., 2016. Volatile fatty acids (VFAs) production from swine manure through short-term dry anaerobic digestion and its separation from nitrogen and phosphorus resources in the digestate. Water Res. 90, 344–353.
Jorfi, S., Pourfadakari, S., Kakavandi, B., 2018. A new approach in sono-photocatalytic degradation of recalcitrant textile wastewater using MgO@Zeolite nanostructure under UVA irradiation. Chem. Eng. J. 343, 95–107.
Kato, S., Chino, K., Kamimura, N., Masai, E., Yumoto, I., Kamagata, Y., 2015. Methanogenic degradation of lignin-derived monoaromatic compounds by microbial enrichments from rice paddy field soil. Sci. Rep. 5, 14295.
Khan, M.D., Khan, N., Nizami, A.-S., Rehan, M., Sabir, S., Khan, M.Z., 2017. Effect of co-substrates on biogas production and anaerobic decomposition of pentachlorophenol. Bioresour. Technol. 238, 492–501.
Li, F., Huang, J., Xia, Q., Lou, M., Yang, B., Tian, Q., Liu, Y., 2018. Direct contact membrane distillation for the treatment of industrial dyeing wastewater and characteristic pollutants. Sep. Purif. Technol. 195, 83–91.
Liu, X.-W., Chen, J.-J., Huang, Y.-X., Sun, X.-F., Sheng, G.-P., Li, D.-B., Xiong, L., Zhang, Y.-Y., Zhao, F., Yu, H.-Q., 2014. Experimental and theoretical demonstrations for the mechanism behind enhanced microbial electron transfer by CNT network. Sci. Rep. 4, 3732.
Lu, X., Ni, J., Zhen, G., Kubota, K., Li, Y.-Y., 2018. Response of morphology and microbial community structure of granules to influent COD/SO_4^{2-} ratios in an upflow anaerobic sludge blanket (UASB) reactor treating starch wastewater. Bioresour. Technol. 256, 456–465.
Manenti, D.R., Soares, P.A., Silva, T.F.C.V., Modenes, A.N., Espinoza-Quinones, F.R., Bergamasco, R., Boaventura, R.A.R., Vilar, V.J.P., 2015. Performance evaluation of different solar advanced oxidation processes applied to the treatment of a real textile dyeing wastewater. Environ. Sci. Pollut. Res. 22 (2), 833–845.
Mulkidjanian, A.Y., Makarova, K.S., Galperin, M.Y., Koonin, E.V., 2007. Inventing the dynamo machine: the evolution of the F-type and V-type ATPases. Nat. Rev. Microbiol. 5, 892.
Schultrich, K., Frenzel, F., Oberemm, A., Buhrke, T., Braeuning, A., Lampen, A., 2017. Comparative proteomic analysis of 2-MCPD- and 3-MCPD-induced heart toxicity in the rat. Arch. Toxicol. 91 (9), 3145–3155.
Teng, J., Shen, L., He, Y., Liao, B.-Q., Wu, G., Lin, H., 2018. Novel insights into membrane fouling in a membrane bioreactor: Elucidating interfacial interactions with real membrane surface. Chemosphere 210, 769–778.
Wen, Y.-Z., Tong, S.-P., Zheng, K.-F., Wang, L.-L., Lv, J.-Z., Lin, J., 2006. Removal of terephthalic acid in alkalized wastewater by ferric chloride. J. Hazard. Mater. 138 (1), 169–172.
Wijetunga, S., Li, X.-F., Jian, C., 2010. Effect of organic load on decolourization of textile wastewater containing acid dyes in upflow anaerobic sludge blanket reactor. J. Hazard. Mater. 177 (1), 792–798.
Xu, H., Liu, Y., Gao, Y., Li, F., Yang, B., Wang, M., Ma, C., Tian, Q., Song, X., Sand, W., 2018. Granulation Process in an Expanded Granular Sludge Blanket (EGSB) Reactor for Domestic Sewage Treatment: Impact of Extracellular Polymeric Substances Compositions and Evolution of Microbial Population. Bioresour. Technol. 269, 153–161.
Yan, Z., Joshi, P., Gorski, C.A., Ferry, J.G., 2018. A biochemical framework for anaerobic oxidation of methane driven by Fe(III)-dependent respiration. Nat. Commun. 9, 1642.
Yang, B., Xu, H., Wang, J., Song, X., Wang, Y., Li, F., Tian, Q., Ma, C., Wang, D., Bai, J., Sand, W., 2017. Bacterial and archaeal community distribution and stabilization of anaerobic sludge in a strengthen circulation anaerobic (SCA) reactor for municipal wastewater treatment. Bioresour. Technol. 244, 750–758.
Yang, B., Xu, H., Wang, J., Yan, D., Zhong, Q., Yu, H., 2018a. Performance evaluation of anaerobic baffled reactor (ABR) for treating alkali-decrement wastewater of polyester fabrics at incremental organic loading rates. Water Sci. Technol. 77 (10), 2445–2453.
Yang, B., Xu, H., Yang, S., Bi, S., Li, F., Shen, C., Ma, C., Tian, Q., Liu, J., Song, X., Sand, W., Liu, Y., 2018b. Treatment of industrial dyeing wastewater with a pilot-scale strengthened circulation anaerobic reactor. Bioresour. Technol. 264, 154–162.
Ye, J.-S., Liu, J., Li, C., Zhou, P., Wu, S., Ou, H., 2017. Heterogeneous photocatalysis of tris(2-chloroethyl) phosphate by UV/TiO2: Degradation products and impacts on bacterial proteome. Water Res. 124, 29–38.
Ye, J., Zhou, P., Chen, Y., Ou, H., Liu, J., Li, C., Li, Q., 2018. Degradation of 1H-benzotriazole using ultraviolet activating persulfate: Mechanisms, products and toxicological analysis. Chem. Eng. J. 334, 1493–1501.
Zhang, H., Li, Q., Wang, L., Chen, Y., 2018a. Investigation of structure and function of mitochondrial alcohol dehydrogenase isozyme III from Komagataella phaffii GS115. *Biochimica et Biophysica*. Acta (BBA) – General Subjects 1862 (5), 1199–1208.
Zhang, M., Hong, H., Lin, H., Shen, L., Yu, H., Ma, G., Chen, J., Liao, B.-Q., 2018b. Mechanistic insights into alginate fouling caused by calcium ions based on terahertz time-domain spectra analyses and DFT calculations. Water Res. 129, 337–346.
Zhang, M., Lin, H., Shen, L., Liao, B.-Q., Wu, X., Li, R., 2017. Effect of calcium ions on fouling properties of alginate solution and its mechanisms. J. Membr. Sci. 525, 320–329.
Zhao, H.-Q., Liu, Q., Wang, Y.-X., Han, Z.-Y., Chen, Z.-G., Mu, Y., 2018. Biochar enhanced biological nitrobenzene reduction with a mixed culture in anaerobic systems: Short-term and long-term assessments. Chem. Eng. J. 351, 912–921.